Synthesis of Drowning-Out Crystallization-Based Separations

David A. Berry, Susan R. Dye, and Ka M. Ng
Dept. of Chemical Engineering, University of Massachusetts, Amherst, MA 01003

A method is presented to synthesize drowning-out crystallization-based separation schemes for binary mixtures. The method tracks how the composition of each process stream changes from unit to unit on a phase diagram by assuming that the system is at equilibrium. Features of phase behavior favorable to drowning-out processes are identified. Two types of systems are highlighted. In the first, the drowning-out agent causes the solute to become sparingly soluble. Several process alternatives to separate the feed into pure components are proposed. Dominant costs of each configuration are identified. In the second, the solute is extracted into a phase rich with respect to the drowning-out agent. The extraction can be performed in a decanter, countercurrent extractor, or fractional countercurrent extractor. Guidelines are given to select an extractor type and to choose between crystallizer-extractor and extractor-crystallizer equipment trains.

Introduction

Drowning-out crystallization relies on the addition of an extraneous component to effect a separation. This component may be a gas, a liquid, a supercritical fluid, or a solid and is often referred to as an antisolvent, diluent, drowning-out agent, precipitant, salting-out, solventing-out, or watering-out agent. We refer to this component as the drowning-out agent. Like all crystallization processes, drowning-out can separate components that are difficult to distill. In addition, it offers two advantages over other crystallization techniques that rely on evaporation or temperature swings to obtain crystals. It is particularly suitable for the separation of heat-sensitive materials because crystallization can often occur at or near ambient temperatures. The technique also provides a route to increase the yield of components whose solubility varies relatively little with temperature. For these reasons, drowning-out is widely used in the manufacture of pharmaceuticals and agrochemicals as well as other fine chemicals.

In contrast, there are only a limited number of examples of its use in large-scale commercial processes. Perhaps one of the most important examples is the production of cellulose triacetate, which is precipitated from an acetic-acid solution by adding water as the drowning-out agent. Another example is found in the production of terephthalic acid, which is precipitated from a mixture of pressurized air, para-xylene, acetic acid, and catalyst (Bemis et al., 1982). A process of potential significance is described in a patent by Hanson and Lynn (1989) to solution-mine sodium chloride. In this process, water is used to dissolve the salt from mineral deposits. An amine is used as the drowning-out agent. The flow sheet consists of an extractor, a crystallizer, among others. By operating these units at different temperatures, crystals of the salt and a stream of almost pure water are obtained. The water is returned to the mine to dissolve more salt. The flow sheet is designed so that the drowning-out agent is continuously recycled within the process.

Most of the literature about drowning-out crystallization is focused on laboratory-scale experiments of aqueous salt solutions. For example, de Bruyn (1900) proposed schemes to separate alcohol–salt–water systems. Alfassi (1984) studied separating electrolytes from aqueous solutions. Jagadesh et al. (1992) studied the crystallization of potassium chloride by an ammoniation process. Lozano and Wint (1982) examined the production of potassium sulfate catalyzed by aqueous ammonia. Weingaertner et al. (1991) recovered sodium carbonate from water with 1-propanol. Mydlarz and Jones (1991) studied the agglomeration kinetics during batch drowning-out precipitation of potash alum with aqueous acetone.

Drowning-out crystallization is frequently viewed as a difficult separation technique for a number of reasons. It is often troublesome to control the level of supersaturation and, as a

Correspondence concerning this article should be addressed to K. M. Ng.

result, very fine crystal slurries are obtained. Jones and Mydlarz (1990) showed that despite this possibility, careful control of operating conditions can give crystal products close in filterability to those produced by cooling crystallization. Also, improved models and control algorithms are available for particle-size control (Farrell and Tsai, 1995). Another obstacle is the absence of screening procedures for the selection of suitable drowning-out agents. Search procedures developed for solvent selection in liquid–liquid extraction should provide a good starting point. Pretel et al. (1994) gave a systematic procedure to predict physical and equilibrium properties, and solvent performance. Macchietto et al. (1990) described how to search for solvents by a group contribution molecular design approach.

Furthermore, little information is available for the conceptual design of drowning-out crystallization processes. Recently, methods have been developed for the conceptual design of other crystallization-based separation processes. Rajagopal et al. (1991) and Dye and Ng (1995a) discussed the use of extractive crystallization to completely separate binary and ternary systems, respectively. A similar approach was taken for the conceptual design of fractional crystallization processes (Rajagopal et al., 1988; Dye and Ng, 1995b; Berry and Ng, 1996). Ng (1991) provided a systematic method to separate a multicomponent mixture of molecular solids.

This article gives a method to synthesize drowning-out crystallization processes for separating binary mixtures. First, we discuss the phase behavior encountered in drowning-out crystallization processes. Second, we propose several flowsheet structures for effecting separations. The advantages and trade-offs of each configuration are given and guidelines are also proposed for the selection of flow-sheet structures.

Description of Phase Behavior

Understanding phase diagrams is critical to the synthesis of crystallization-based separation processes. Before proceeding with a discussion of specific process flow sheets, we give an overview of the features of phase behavior encountered in drowning-out crystallization separations. Since the separation processes that follow are all from ternary systems, the discussion is restricted to ternary phase diagrams.

The Gibbs phase rule for condensed isothermal systems specifies that the degrees of freedom for a ternary system is $(3 - P)$ where P is the number of phases. Examples of ternary phase diagrams that have one, two, and three coexisting phases are given in Table 1.

Figure 1a gives examples of ternary isobaric, isothermal phase diagrams with a maximum of two coexisting phases. The compositions where two phases coexist have one degree of freedom and are represented as a curve on the diagram. The vertices A, B, and D represent the pure solvent, solute, and drowning-out agent, respectively. Diagram (a) has only solid–liquid equilibrium. Diagrams (b) through (e) have both solid–liquid and liquid–liquid equilibrium. The compositions of liquids L_1 and L_2 give the solubility of B in pure A and D, respectively. Curve L_1L_2 gives the solubility of B for all mixtures of A and D. Regions marked by $(B + L)$ and lightly shaded, like L_1BL_2, represent liquid coexisting with solid B. Unshaded regions, like L_1AL_2D, represent homogeneous liquids. Diagram (b) has one partially miscible pair. A and B as well as B and D are completely miscible. Composition L_3 gives the miscibility of D in A, and composition L_4 gives the miscibility of A in D. Curve L_3L_4 is the miscibility of the two liquids for any composition on the diagram. Point P is a plait point. Regions marked by $(L + L)$ and that are darkly shaded, like L_3PL_4, indicate compositions where two liquids coexist. Diagrams (c) and (d) both have two partially miscible pairs. However, diagram (c) has one coexistence envelope that spans the distance from the AD edge to the BD edge of the diagram. Liquids L_5 and L_6 are the miscibility of D in B and B in D, respectively. Diagram (d) has two coexistence curves. This system possesses two plait points. Diagram (e) shows an island-type miscibility gap. All the binary pairs of

Table 1. Examples of Ternary Phase Diagrams As Depicted in Figure 1

A	*B*	*D*	*T* (°C)	Diagram	Reference
Water	Potassium chloride	2-Propanol	25	a	Gomis et al. (1994)
Water	Disodium sulfate	Methanol	40	a	Mersmann and Kind (1988)
Methanol	Urea	Carbon dioxide	25	a**	Francis (1954)
n-Heptane	3,5-Xylenol	Carbon dioxide	25	a**	Francis (1954)
Acetone	Mercuric chloride	Carbon dioxide	25	a**	Francis (1954)
Acetic acid	Acetamide	Carbon dioxide	25	b**	Francis (1954)
Water	Sodium hydroxide	Butanol	25	b	Zepeda et al. (1979)
Toluene	Maleic anhydride	Propylene glycol	25	b	Francis (1965a)
Heptane	Sulfur	Ammonia	25	b*	Francis (1965b)
Water	Disodium sulfate	Poly(ethylene glycol)	28	b	Ho-Gutierrez et al. (1994)
Glycerol	*p*-Toluidine	Carbon dioxide	25	c**	Francis (1954)
Succinonitrile	Benzene	Carbon dioxide	25	d**	Francis (1954)
Propane	Methanol	Sulfur dioxide	25	e†	Francis (1965c)
Water	Sodium chloride	Ethylacetate	30	f	Gomis et al. (1993)
1,4-Dioxane	Copper (II) chloride	Methanol	30	f	Dorn et al. (1965)
Water	Sodium chloride	2-Propanol	25	g	Gomis et al. (1994)
Water	Sodium chloride	Potassium chloride	25	h	Zemaitis et al. (1986)

*Phase of ammonia is liquid.
**Phase of carbon dioxide is liquid. Diagrams were measured at a pressure of 65 atm.
†Phase of sulfur dioxide is liquid. SLE is absent at listed conditions.

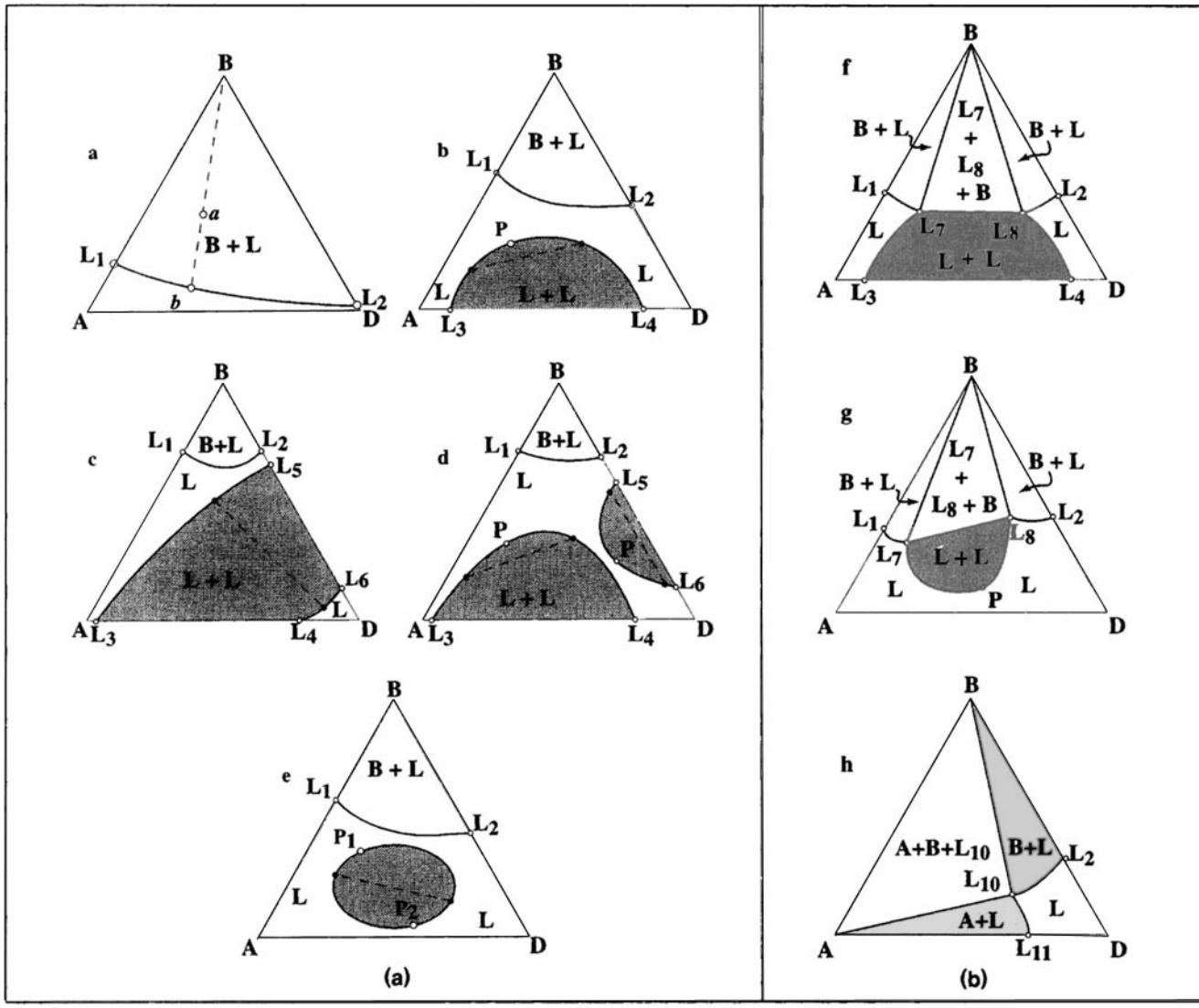

Figure 1. Examples of ternary phase diagrams with: (a) one or more degrees of freedom at all compositions; (b) zero degree of freedom at one or more compositions.

pure components are completely miscible in each other. A region of immiscibility exists within the interior of the phase diagram. There are two plait points, P_1 and P_2.

Tie lines on the diagrams are represented as dashed lines. A tie line between a pure solid and a liquid is drawn from the respective vertex to the solid–liquid coexistence curve. For example, a system with overall composition given by point a on diagram a is composed of pure B and a liquid given by point b. The relative masses of the phases are determined by the lever rule. An examination of the phase diagrams reveals that the distribution coefficient can be greater than or less than unity. Tie lines for these cases are shown in diagrams b and e, respectively. Systems where the distribution coefficient is both less and greater than unity within the phase envelope exhibit solutropy.

Figure 1b gives examples of phase diagrams with three coexisting phases. The compositions on isobaric, isothermal phase diagrams with three coexisting phases have zero degrees of freedom and are represented as points. In diagrams f and g these regions consist of liquid–liquid–solid equilibrium and are indicated by the area bounded in triangle L_7BL_8. Any composition in this region splits into liquids L_7, L_8 and solid B. In diagram h the region of zero degrees of freedom consists of solid–solid–liquid equilibrium. Any composition within triangle $BL_{10}A$ splits into solid B, A, and liquid L_{10}.

Much work has been done to predict heterogeneous phase equilibrium. Pham and Doherty (1990) presented a simple procedure for calculating liquid–liquid–vapor phase equilibrium for systems with a maximum of two coexisting liquid phases. Zerres and Prausnitz (1994) gave a semiempirical thermodynamic method to establish a framework for calculating liquid–liquid equilibrium in ternary systems containing water, an organic solvent, and a salt. Various models are available for calculating the solubilities of inorganics in solution (Zemaitis et al., 1986). Zhu et al. (1990) presented a method to calculate the liquid–solid and liquid–liquid equilibrium behavior of antibiotics. McBride and Brennecke (1993) provided a model for the solid–liquid solubilities of solvating species. Kolker (1991) developed equations that can

be used to determine extraction distribution ratios and solubility of substances in high concentrations.

Synthesis of Separation Schemes

In the following discussion, we show which of the phase behaviors from Figure 1 are most suited to separation by drowning-out crystallization. The separations can be grouped into two general classes based upon how D affects the phase behavior. In Class I separations, D is used to increase the per-pass yield of B by decreasing the solubility of B. In Class II separations, the drowning-out agent induces a liquid–liquid phase split. Both classes recover crystals of B. Component A can be recovered either as a solid or a liquid at a specified purity.

Class I separations

The simplest Class I process consists of adding D to selectively crystallize B and purging the crystallizer effluent. Figure 2 shows a system where D has limited solubility in A. The figure also shows a polythermal phase diagram, isothermal cuts of the phase diagram at the operating temperatures of the mixing tank (T_m) and crystallizer (T_c), and the process flow sheet. The numbers in the phase diagram correspond to the stream numbers in the flow sheet. The process proceeds as follows. The feed (F) is combined with the drowning-out agent in a mixing tank ($M1$) to make stream 1. The mixing tank is operated at T_m. The stream is fed to the crystallizer ($C1$). Even though D is insoluble in A at some compositions, the amount of D added has been chosen so that only B crystallizes. The solid B is filtered from the system. Although the yield of B can be increased by operating at the double saturation point, the composition of stream 2 is chosen not to be doubly saturated in order to provide a safety margin from coprecipitation of D and B. The crystallizer effluent is purged.

The design variables for this process are easily identified by solving the appropriate design equations. The solubility of B in the crystallizer is set by specifying T_c and the mass fraction of one of the components in stream 2. We choose to specify $x_{D,2}$. Another design variable is T_m. Design variables associated with the filter and the dryer are not considered.

In most cases it is desirable to recycle the drowning-out agent and recover both A and B. One process alternative is to crystallize both A and B. Figure 3 gives a Jänecke projection of the polythermal phase diagram and an isothermal phase diagram, along with process paths drawn on these diagrams, and the equipment configuration. The composition of stream 3 and either the temperature or the amount of D at each crystallizer are the design variables. The process pro-

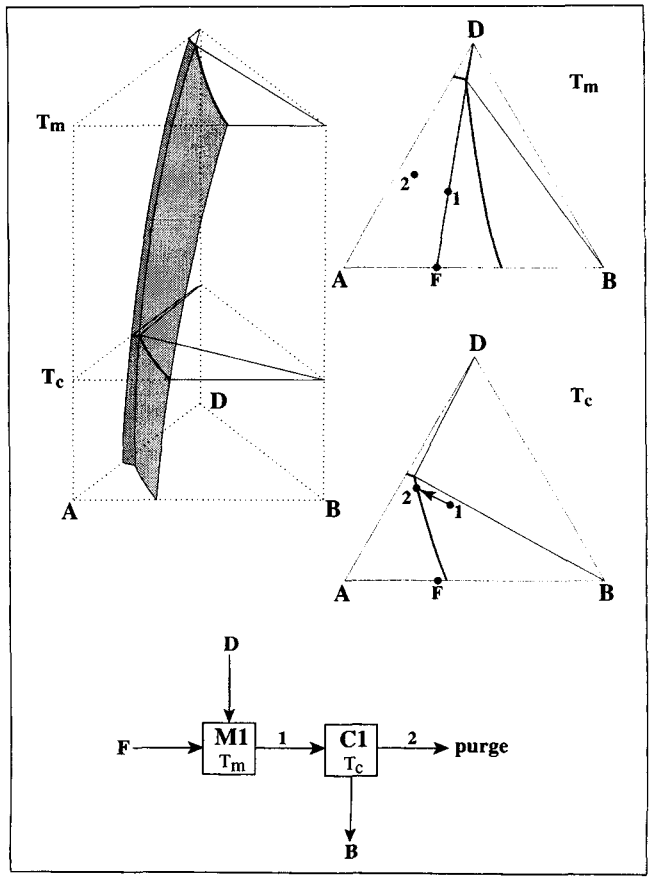

Figure 2. Base case design with a purge stream.

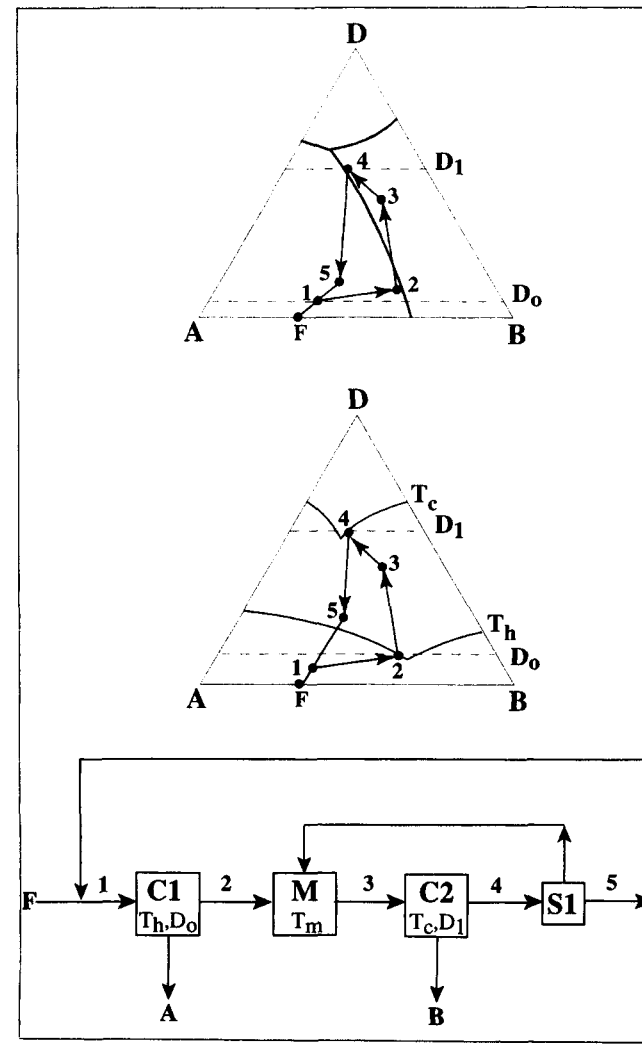

Figure 3. Process alternative crystallizing both *A* and *B*.

ceeds as follows. The feed and stream 5 are combined and heated to a temperature that keeps the stream unsaturated. Stream 1 is fed into $C1$, which operates at T_h and contains D_0. Since the composition lies in a region supersaturated with A, component A crystallizes and is filtered from the system. The crystallizer effluent (stream 2) is combined with recycled D in mixing tank M. The temperature of the mixing tank (T_m) is chosen to keep the stream unsaturated. Stream 3 is fed to $C2$. This crystallizer operates at T_c and D_1. At these conditions, the stream is supersaturated with B. Component B crystallizes and is filtered from the system. The crystallizer effluent is sent to a unit ($S1$), which separates some of the D from the stream. The D-rich stream is recycled to M. The D-lean stream, stream 5, is recycled to the feed. This process alternative as well as the associated process economics is discussed explicitly by Rajagopal et al. (1988), and Dye and Ng (1995a,b).

Figure 4 shows the process alternative that distills the crystallizer effluent to separate A from D. The polythermal solid–liquid phase diagram, isothermal cuts at T_c and T_m, and the process flow sheet are given. In this system, D greatly decreases the solubility of B. Above 50% D, B is sparingly soluble. At all compositions, D is completely soluble in A. The process proceeds exactly as in the previous example (Figure 2); however, stream 2 is sent to a distillation column ($S1$) to separate A from the crystallizer effluent. The distillate (stream 3) and makeup D are combined and recycled to the mixing tank.

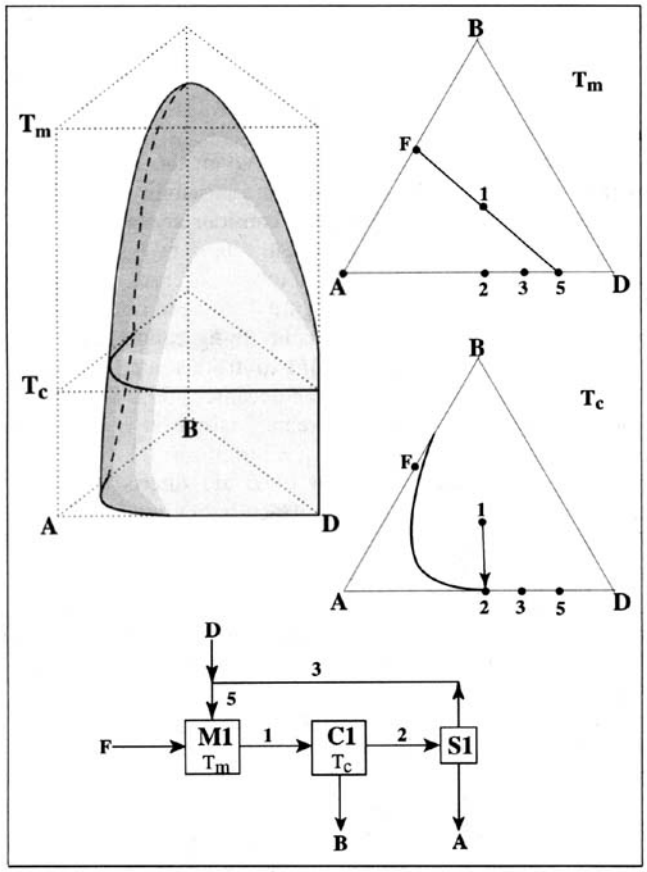

Figure 4. Process alternative regenerating *D* by distillation.

Table 2. Input Parameters for Class I Separations

F	5 ton/d
$x_{B,F}$	0.55
Cp_{solution}	2.59 kJ/kg
ΔH_{cryst}	167 kJ/kg
T_c	42°C
T_m	77°C
T_{sat}	100°C
α	1.5
$\Delta H_{\text{vap},D}$	703 kJ/kg
Value of B	\$2.20/kg
Value of D	\$0.22/kg
\$ steam	\$5.5/1,000 kg
$x_{D,\text{bottoms}}$	0.02
$x_{D,\text{distillate}}$	0.79
Solubility Relationship	
$x_{B,\text{sat}} = 0.5910 - 1.866^* x_{D,2} + 1.855^* x_{D,2}^2 - 0.5743^* x_{D,2}^3$	

Shortcut design procedures for three-component distillation columns are reviewed by Fien and Liu (1994), among others. In this example, B is nonvolatile and A and D are the heavy and light keys, respectively; however, the success of the separation does not depend on this assignment of keys. We further assume that there are no azeotropes or pinch points to complicate distillation. The feed is a saturated liquid. The bottoms is rich in A with trace amounts of B and D. The compositions of the crystallizer effluent, the distillation column bottoms, and the distillate are design variables.

In our cost calculations we assume that refrigeration is not required for the crystallizer. The major capital costs are due to the crystallizer, distillation column, and heat exchanger to heat stream 2. The utility costs are due to cooling water and steam for the reboiler and the heat exchangers. The parameters used to cost the process are given in Table 2. The values given for $x_{D,\text{bottoms}}$ and $x_{D,\text{distillate}}$ are the optimal compositions of the column bottoms and distillate. Cost models are those given in Douglas (1988). The total annual cost (TAC) is the sum of the utility costs and the capital costs with a charge factor of 1/3 year. We choose to set the composition of stream 2 by specifying the fraction of D.

These cost calculations reveal the economic trade-offs to this process. Figure 5 shows that as $x_{D,2}$ increases, the TAC increases monotonically. As $x_{D,2}$ increases, the process flows increase, resulting in larger equipment and heating loads. The process cost (PC) is calculated by adding the TAC to the value of B and D lost in the bottoms. The lower the process cost, the more favorable the process economics become. The process cost reaches a minimum (PC_{min}) when $x_{D,2}$ equals 0.69, and is caused by a trade-off between the costs covered in the TAC and decreasing costs due to loss of B and D as $x_{D,2}$ increases. Notice that the PC_{min} occurs approximately where there is complete recovery of B. The fraction of annual costs due to steam is low at all compositions of $x_{D,2}$.

Figure 6 is a process alternative when A and D are the light and heavy keys, respectively. In this configuration, vapor (stream 3) is removed from the crystallizer and sent to a dual feed distillation column. The compositions of crystallizer effluent, bottoms, and distillate are design variables. Notice that as a result of evaporating a mixture rich in A from the crystallizer, the compositions of streams 1 and 2, and vertex B are no longer collinear.

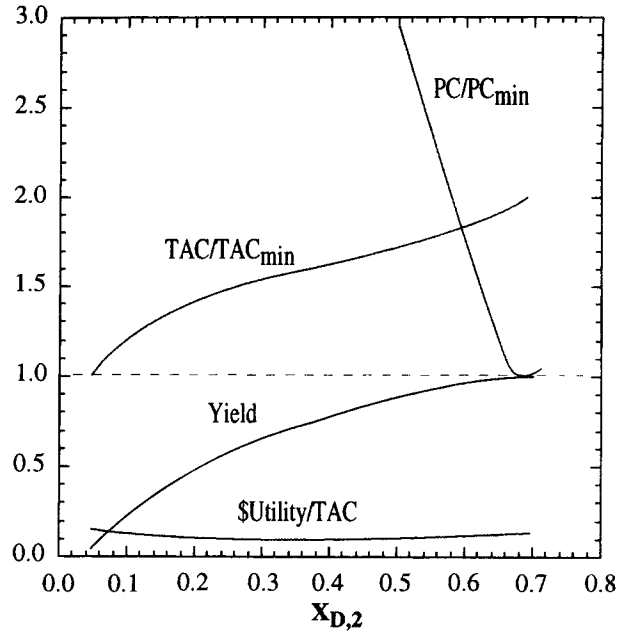

Figure 5. Process economics of regenerating *D* by distillation as a function of the composition of the crystallizer effluent.

Class II separations

When the yield of product is low or when annual costs are prohibitively high for a Class I separation scheme, Class II separations can provide an attractive alternative. Class II separations utilize a miscibility gap to extract B into a D-rich phase using a decanter, countercurrent extractor, or a fractional countercurrent extractor. Which equipment configuration will prove most economical for a given system depends on the phase behavior of the system, the value of its products, and the composition of the feed. Design procedures for extraction columns can be found elsewhere. For example, many graphical approaches to extractor design are described in Lo et al. (1983). Leonard et al. (1990) proposed a model for analyzing solvent extraction processes carried out in any type of column. Minotti et al. (1996) used a geometric approach to calculate the minimum solvent flows in multistage countercurrent extractors.

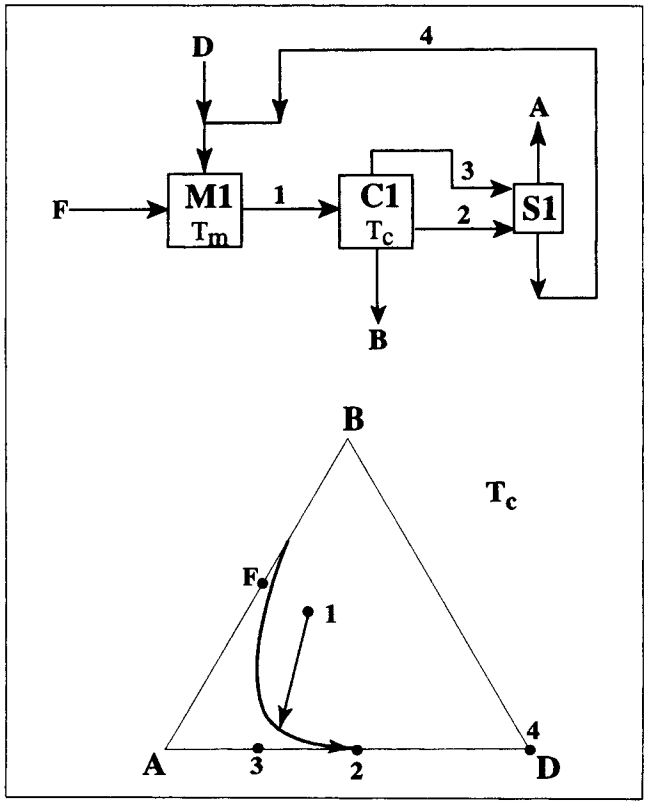

Figure 6. Process alternative with evaporative crystallization.

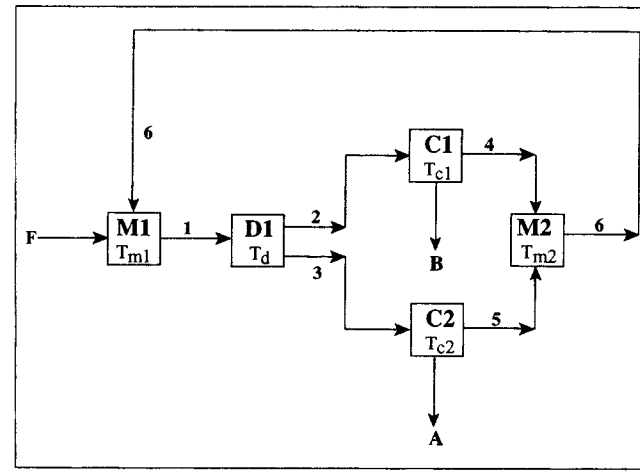

Figure 7. Process alternative crystallizing both *A* and *B* with phase split.

Recovery of Crystals of A and B. When the melting temperatures of A and B are close and a miscibility gap can be created near the melting surfaces, consider crystallizing both components. Such a configuration offers two advantages. First, pure A and B are completely recovered. Second, in contrast to the case shown in Figure 4, D need not be vaporized. Figure 7 gives the equipment configuration. The feed and stream 6 are combined in $M1$ to make stream 1. Stream 1 is unsaturated and is fed into the decanter ($D1$). The stream splits into two liquid phases. Stream 2 is rich in B. It is sent to $C1$, which is operated at T_{c1}. Crystallizer $C1$ supersaturates stream 2 with B. Crystals of B are filtered from the system. Stream 3 is sent to $C2$, which is operated at T_{c2}. In $C2$ the stream becomes supersaturated with A. Crystals of A are filtered from the system. Both crystallizer effluents, streams 4 and 5, are combined in $M2$. Stream 6 is unsaturated and is recycled to $M1$. The design variables are the temperatures of the crystallizers, the decanter, and the mixing tanks.

Figure 8 shows a phase diagram for this separation as well as isothermal cuts of the phase diagram at the decanter and crystallizer temperatures. At T_c the system exhibits the familiar solid–liquid phase diagram that involves four distinct areas of equilibrium: a homogeneous liquid, solid A and a liquid, solid B and a liquid, and two solids and a liquid. At T_d, A is a liquid which is partially miscible with D. For this system, both crystallizers are operated at the same temperature.

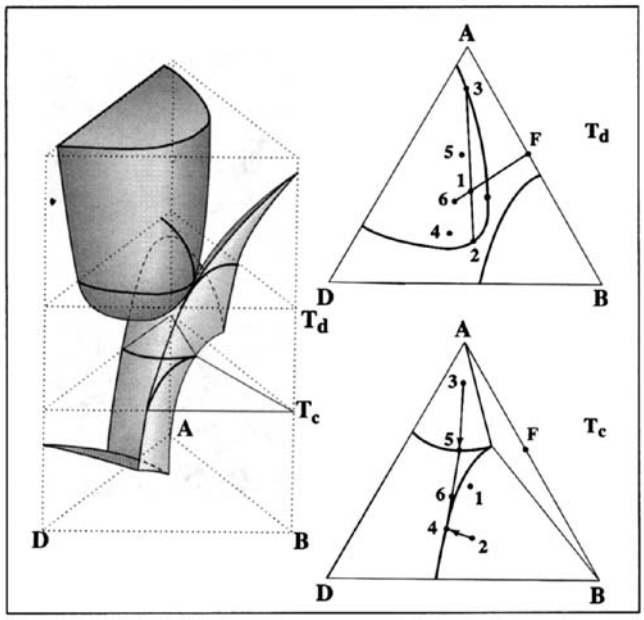

Figure 8. Phase behavior for use with flowsheet to recover crystals of *A* and *B* with phase split.

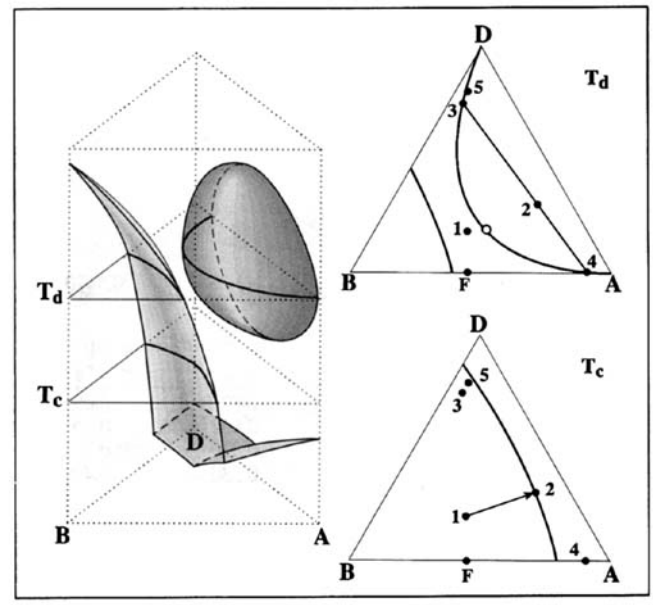

Figure 10. Phase behavior for use with flowsheet crystallizing *B* and then regenerating *D* with a decanter.

Recovery of A as a Liquid and B as a Solid. Figure 9 gives the base equipment configuration to crystallize B and regenerate the drowning-out agent with a decanter. The process proceeds as follows. The feed and stream 5 are combined in a mixing tank ($M1$). The operating temperature of the tank (T_m) is chosen so that stream 1 is unsaturated. Stream 1 is fed to the crystallizer ($C1$), which operates at a temperature (T_c). The change in temperature causes the stream to become supersaturated with B. The crystals of B are filtered from the process. The crystallizer effluent is sent to a decanter ($D1$) that splits the stream into one rich in D (stream 3) and another rich in A (stream 4). Stream 4 is purged. Stream 3 is recycled and combined with fresh solvent to make stream 5. The amount of D added to stream 3 equals the amount lost in the purge.

Figure 10 tracks the composition changes of the separation described earlier on a phase diagram. It shows a polythermal phase diagram as well as the process paths and stream compositions drawn on isothermal cuts at T_d and T_c. The system exhibits upper and lower critical solution temperatures. At T_d there is a region where B is insoluble and where the solution splits into two phases. At T_c, there is a region of solid–liquid equilibrium, but there is no miscibility gap. The isothermal cut at T_m is omitted on the polythermal phase diagram to maintain the clarity of the figure.

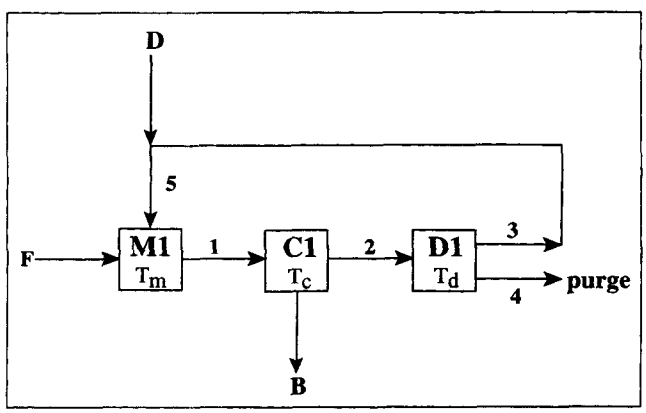

Figure 9. Flowsheet crystallizing *B* and then regenerating *D* with a decanter.

The design variables for this process are T_m, T_c, and T_d. The composition of stream 2 is also a design variable. The constraint on the composition of stream 2 is that it must lie on the solubility curve for B at T_c but within the immiscibility envelope at T_d.

The major capital costs of this equipment configuration are those for the crystallizer and the heat exchangers. The major utility costs come from the steam to heat the process flows to T_d. One advantage of a Class II over a Class I separation that requires a distillation column is that it may have lower capital requirements and utility costs. The annual costs for a decanter should be much lower than those for a distillation column because heat to vaporize D in the regenerator need not be supplied. Table 3 gives the data for the solubility and miscibility curves shown in Figure 10.

As in the Class I separation described previously, the economics of this process can be dominated by the costs associated with loss of B and D. Figure 11 gives the annual cost as a function of the crystallizer effluent composition. The input parameters of the calculations are given in Table 3. The TAC increases as $x_{D,2}$ increases due to larger flows. The yield of B monotonically increases with $x_{D,2}$. Without the drowning-out agent the theoretical yield is 78%. There is a range for the amount of D within which a phase split occurs. The yield is 87.5% for the minimum amount and improves to 95% with the maximum amount of D. Loss of B dominates the process costs regardless of the amount of drowning-out agent added to the system. Configurations that increase the yield even more by use of multistage extraction are given in the following sections.

Table 3. Input Parameters for Class II Separations

F	5 ton/d
$x_{B,F}$	0.55
T_d	77°C
T_c	40°C
T_m	77°C
ΔT_{lm}	15°C
Value of B	\$2.2/kg
Value of D	\$0.22/kg

Solubility Relationship

$$x_{B,2} = 0.2139 + 0.5038^* x_{D,2} + 1.186^* x_{D,2}^2 - 1.288^* x_{D,2}^3 + 0.5470^* x_{D,2}^4$$

Miscibility Data

Extract Composition		Raffinate Composition	
x_A	x_B	x_A	x_B
0.071	0.207	0.875	0.091
0.235	0.235	0.852	0.107
0.108	0.278	0.810	0.138
0.330	0.400	0.330	0.400

Separations Improved by Multistage Extraction. In the processes described earlier, the flow rates of drowning-out agent are manipulated by a decanter. These flow-rate adjustments are possible when the phase diagram exhibits certain characteristics. Recall the Class II process to recover crystals of both A and B (Figure 7). Three features of the phase diagram in Figure 8 are exploited. First, the miscibility envelope lies over compositions where A and B are insoluble. Second, the tielines allow a phase split that places point 3 and point 2 well into the A and B saturation surfaces, respectively. Third, the effluent compositions of both crystallizers lie well within the immiscibility envelope. Also recall the Class II process to recover B as crystals and A as liquid (Figure 9). Again, three features of the phase diagram in Figure 10 are exploited. First, at the crystallizer temperature, B has a low solubility and A and D are miscible. At the decanter temperature, the solubility of B increases while the miscibility of the liquid phases decreases. Also, at this temperature the miscibility gap is wide so that the raffinate is lean in D. Third, D selectively extracts B well.

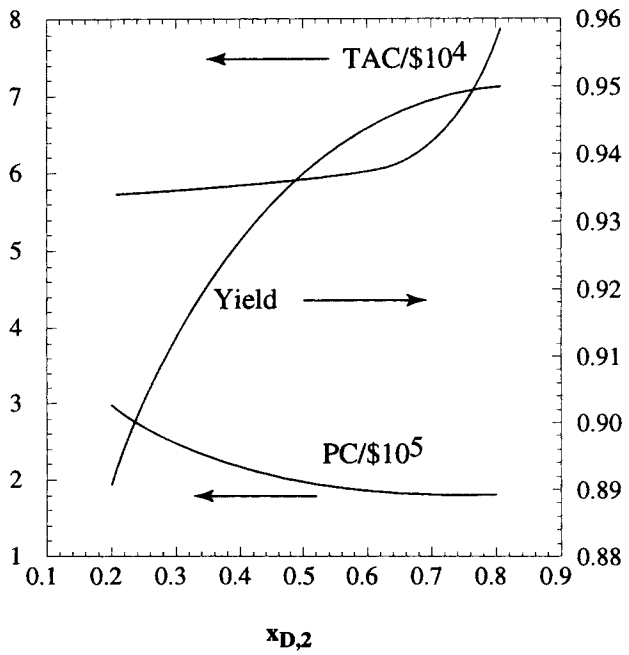

Figure 11. Annual costs and yield of process with decanter.

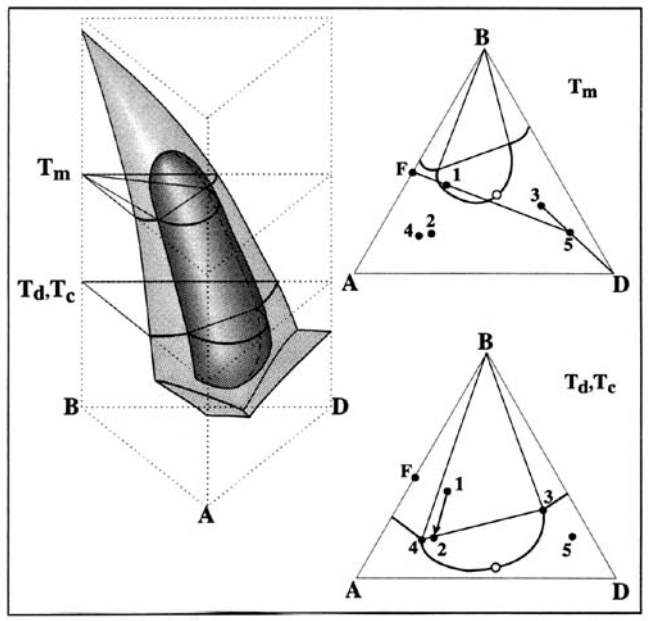

Figure 12. Example of phase behavior where a separation cannot be improved by using multistage extraction.

Often, the phase behavior may not be as favorable to separation by decantation as those listed above. For these systems, different extraction equipment can often be used to improve the feasibility of a separation. Figure 12 shows a system where the immiscibility envelope lies on the B saturation surface. The equipment configuration is the same as that in Figure 9. The difference of this system from that shown in Figure 10 is that the decanter and the crystallizer operate at the same temperature. As can be seen, as the composition of stream 2 is varied, the compositions of stream 4 and stream 3 remain constant; however, the composition of stream 2 does affect the mass ratio of the two streams. Because the composition of stream 4 cannot be affected by stream 2, and B has a high solubility, more B and D are lost in the purge than in the previous example. This separation cannot significantly be improved by using other extraction equipment.

Figure 13 shows a system for which the separation can be improved by multistage extraction. Components A and D are partially miscible and the immiscibility envelope lies on the B saturation surface. The crystallizer and the decanter operate at identical temperatures. As in the previous example, the compositions of streams 3 and 4 are fixed by phase behavior; B has a high solubility at point 2, and a great deal of B and D are lost in the purge. The process can be significantly improved if the raffinate composition were close to the pure A vertex. This can be accomplished by using a countercurrent extractor instead of a decanter.

Replacement of Decanter with Countercurrent Extractor. There are three basic configurations that use a countercurrent extractor. The first distills D from the extract and recycles it to the bottom of the extractor. The second performs

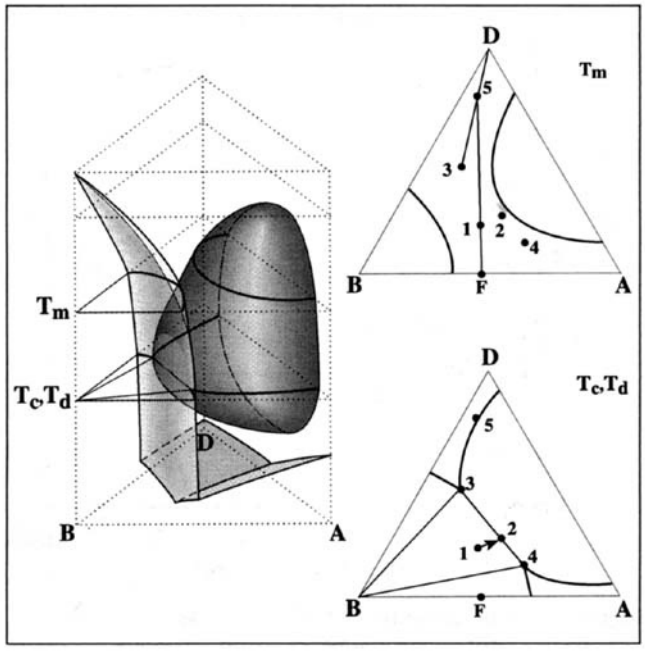

Figure 13. Example of phase behavior where a separation can be improved by using multistage extraction.

the extraction step before the crystallization step. The third uses evaporative crystallization.

Figure 14 shows the first configuration. The feed and stream 4 are combined in $M1$. The stream is sent to $C1$, which operates at T_c. At this temperature component B is supersaturated and crystallizes from solution. The crystals are filtered from the system. Stream 2 is sent to the top of the extractor. The extract (stream 3) is distilled in $S1$ to remove a portion of the D in the stream. The stream rich in B is recycled to $M1$. The raffinate, stream 5, may be purged or it may be stripped of D in $S2$. All the recycled D is returned to the

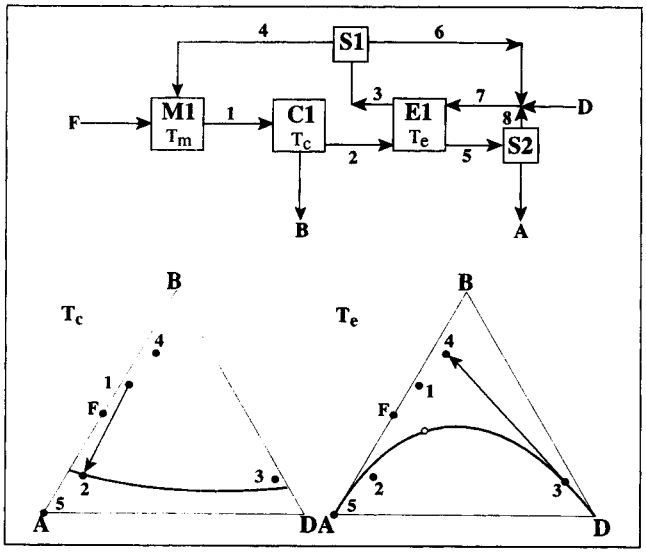

Figure 14. Configuration replacing the decanter with a countercurrent extractor.

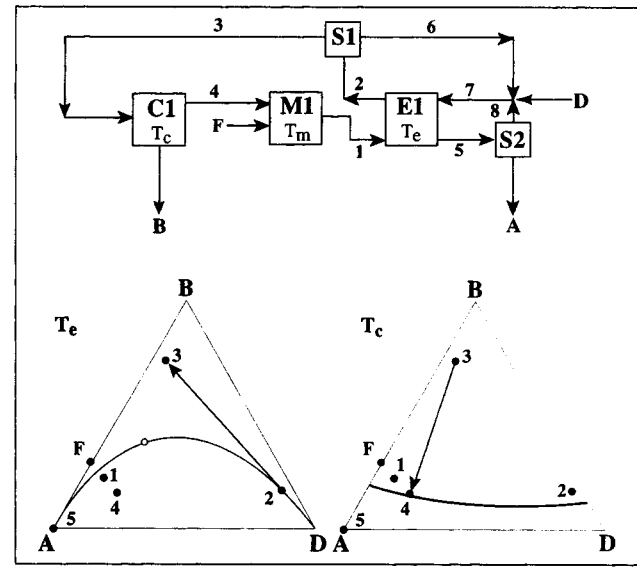

Figure 15. Configuration performing the extraction before the crystallizer.

bottom of the extraction column. The compositions of streams 2, 5, 6 and 8 are design variables. For clarity of presentation, point 5 is assumed to be pure A and points 6, 7 and 8 pure D in the phase diagram.

Figure 15 shows the second configuration. The feed is combined with the crystallizer effluent in a mixing tank to make stream 1. Stream 1 and stream 7 are fed to the top and bottom of the extractor, respectively. The raffinate (stream 5) can be stripped of D in $S2$, which is then recycled to the bottom of the extractor. The extract (stream 2) is sent to a distillation column to regenerate D. The recovered D (stream 6) is recycled to the bottom of the column. Stream 3 is sent to a crystallizer operated at T_c. The flow rate of the drowning-out agent is a design variable. Again, pure A is assumed for stream 5 and pure D for streams 6, 7 and 8.

Comparison of Two Configurations that Use Countercurrent Extraction. The sources of major capital costs for the two configurations are identical. Heat exchangers are required for the crystallizer, extractor, and distillation column. The distillation column and crystallizer are the sources of highest cost. The smallest cost is due to the extractor. The cost of stripping D from the raffinate is not considered. As the fraction of D in the crystallizer effluent increases, process flows increase and larger equipment is required.

Figure 16 compares the costs for the two configurations as a function of the fraction of D in the crystallizer when the fraction of B in the feed is 55%. The yield of B is 99%. The input parameters for the calculation are those given in Table 3. Stream 3 is preheated to 100°C. The temperature of the distillate and bottoms are 80 and 120°C, respectively. We assume the flow of drowning-out agent (streams 2 and 7 in Figures 14 and 15, respectively) is equal to the flow of the feed into the extractor (stream 1). The process costs have been normalized to the minimum process cost for the crystallizer–extractor (*ce*) configuration. The optimal composition of the crystallizer effluent is between 2 and 3% D for the crystallizer–extractor configuration. If a higher purity of D is specified at $S1$, the cost due to distillation increases. At

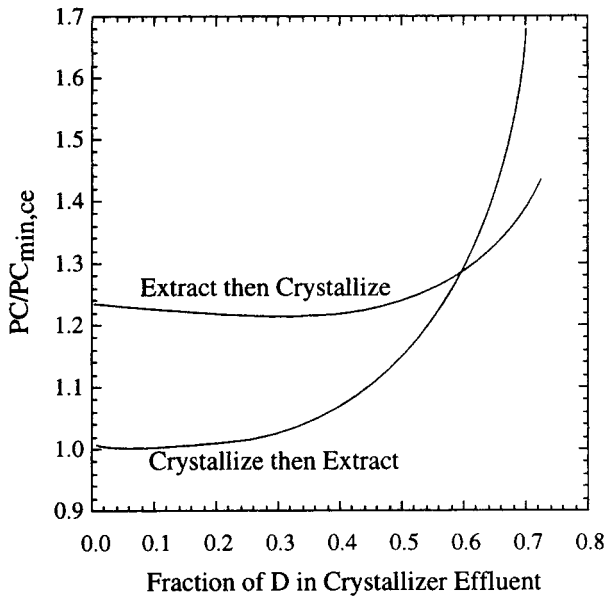

Figure 16. Comparison between countercurrent extraction configurations.

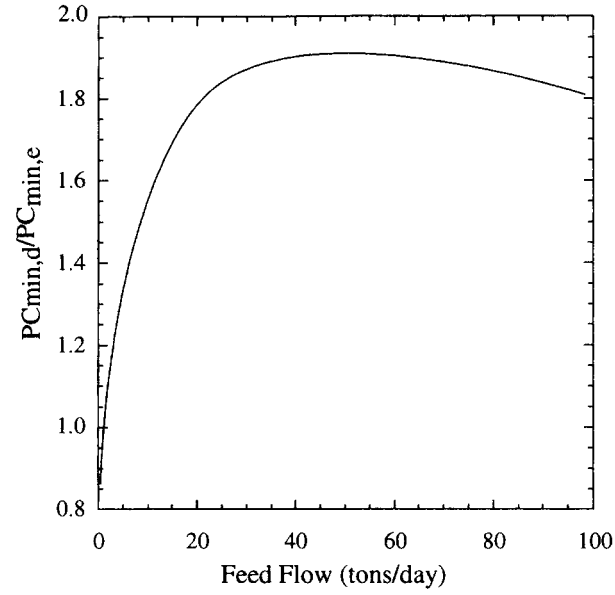

Figure 18. Comparison between process cost of decanter and countercurrent extraction.

higher concentrations of D in crystallizer effluent the process flows require larger equipment sizes. The extractor–crystallizer (ec) configuration is less sensitive to the composition of the crystallizer effluent composition and follows the same trend. The optimal concentration is between 22 and 39% D in the crystallizer effluent.

The composition of the feed impacts the economics of each configuration greatly. Figure 17 compares the minimum process cost of the two configurations as a function of the fraction of B in the feed. For this phase behavior, the extractor–crystallizer configuration is most economical when the feed is less than 28% B. This trend is due to lower flows. The process cost of the multistage extraction configurations can be further improved by optimizing the yield of the product and the flow of drowning-out agent into the extractor. At very high recoveries of B, costs due to the extractor become more dominant.

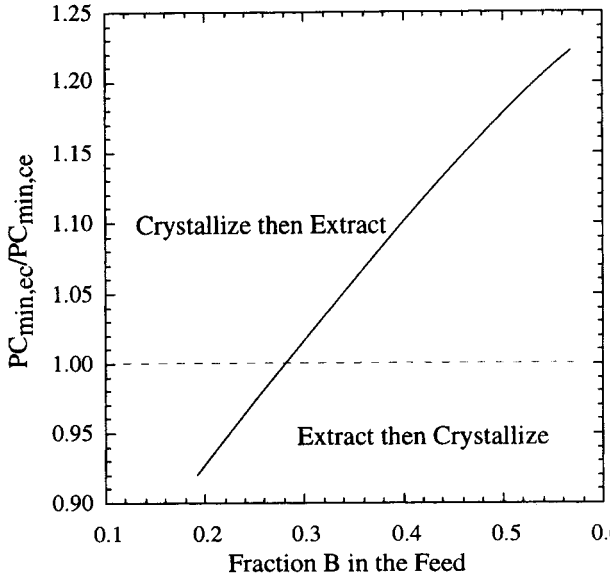

Figure 17. Comparison of process economics of the two countercurrent extraction configurations as a function of feed composition.

Figure 18 compares the process cost for using a decanter to countercurrent extractor as a function of the feed flow rate. The crystallizer precedes the extractor. The composition of the feed is 55% B. As the production rate increases, the decanter configuration costs more due to higher loss of B. For feed flows of 5 and 40 ton/d, multistage extraction improves the economics by 30 and 80%, respectively. Use of countercurrent extraction allows near complete recovery of B. Even at low production rates, the increased annual capital costs are more than made up for by increased yield. At production rates greater than 40 ton/d, the economic improvement for multistage extraction decreases slightly with respect to decantation if the yield is again fixed at 99%. This is because the value of B lost in the bottoms becomes significant compared to the TAC. To maintain the improvement, a higher yield has to be specified.

Another alternative that can be used when A and D are the light and heavy keys, respectively, is to use an evaporative crystallizer to draw off a stream rich in A. Figure 19 shows the flow sheet. Vapor stream 9 and liquid stream 2 are fed into the distillation column. This configuration is expected to have lower process flows than one without an evaporative crystallizer.

Configurations that use countercurrent extraction are most appropriate for phase behavior like that given in Figure 1, diagrams b, c, d and f. These configurations are particularly suited to phase behavior f when B has low solubility. This is because the phase behavior of these systems restricts the extract composition to a maximum B concentration given by L_8. For the other phase behaviors, it is sometimes desirable to further concentrate the extract with respect to B. This can be accomplished by use of fractional countercurrent extraction.

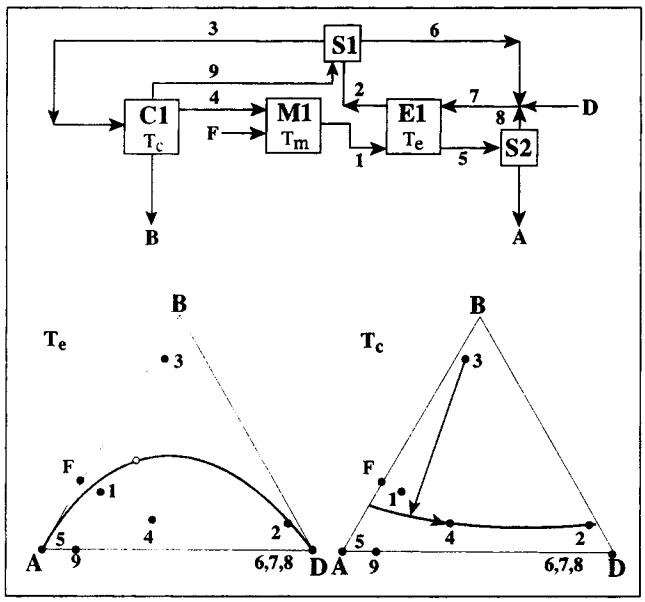

Figure 19. Process alternative with evaporative crystallization.

Use of Fractional Countercurrent Extractor. Use of fractional countercurrent extraction allows the composition of the extract as well as the raffinate to be specified. Figure 20 shows a configuration where the crystallization precedes the extraction. The process proceeds as follows. The feed is combined with stream 8 in a mixing tank. The resulting stream is fed to the crystallizer operated at T_c. B is filtered from the process. The crystallizer effluent is fed into the extractor. The raffinate (stream 4) may be stripped of drowning-out agent to obtain nearly pure A. The extract (stream 5) is distilled. The D recovered from the distillation and stripping is recycled to the bottom of the extraction column. A portion of the distillate (stream 7) is refluxed to the extractor. The remainder (stream 8) is combined with fresh feed. The compositions of streams 2, 4, 5, 9 and 10 are design variables. The reflux ratios for the distillation column and for the extractor are also design variables. For clarity of presentation, nearly pure A is assumed for stream 4 and nearly pure D for streams 6, 9 and 10.

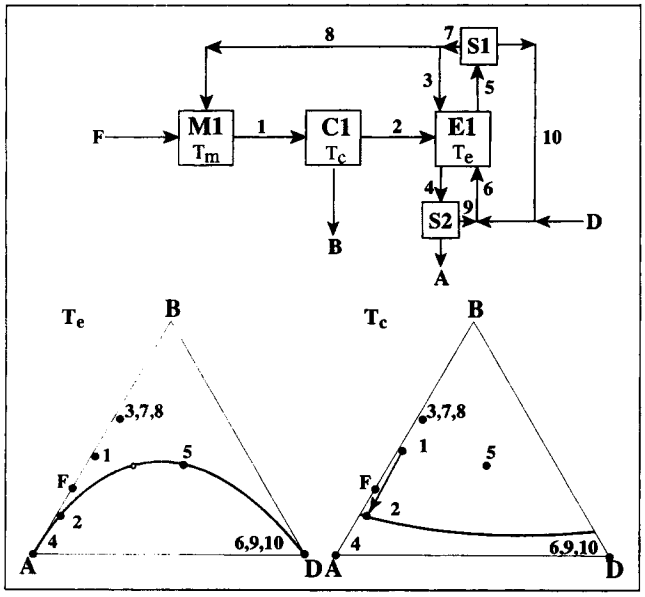

Figure 20. Configuration with fractional countercurrent extraction.

Comparison of Fractional Countercurrent Configurations. Replacing a countercurrent extractor with a fractional countercurrent extractor can reduce the size and costs of the distillation column but also can increase the costs due to the extractor. The column size is reduced when the extract composition is chosen so that less D needs to be vaporized to regenerate the drowning-out agent. The extractor size is increased by additional stages above the feed plate.

There are also other process alternatives. The extractor can precede the crystallizer in the equipment train. When D is the heavy key, use of evaporative crystallization and a dual feed distillation column may reduce capital and utility costs.

Fractional countercurrent extraction should be considered for phase behaviors b, c, and d from Figure 1. As mentioned these phase behaviors are also candidates for countercurrent extraction. For systems where B is easily extracted from A and the drowning-out agent is easy to regenerate by distillation, countercurrent extraction may prove economically superior. Systems in which B is difficult to extract and regeneration of D is costly would benefit most from fractional extraction.

Conclusions

A method is presented for the conceptual design of drowning-out crystallization-based separation processes. Two separation classes are examined. The Class I separation is applied to systems that do not exhibit liquid–liquid equilibrium. The sole purpose of the drowning-out agent is to alter the solubility of one of the solutes. The basic process consisting of a mixing tank and a crystallizer has two alternatives. The first process alternative recovers the solute by crystallization and the solvent and drowning-out agent are purged. In the second, the solute is crystallized and the drowning-out agent is regenerated by distillation. For a high-value product these processes should be designed with minimum product loss in the purge streams.

In Class II separations, a phase split is created to facilitate separation by extraction. For these systems, the drowning-out agent should have low miscibility with the solvent, the solute distribution between the extract and raffinate phases should be high, and the solubility of the solute should be low. When the process can be improved by specification of the raffinate, countercurrent extraction should be considered. When both the composition of the raffinate and extract are required to improve the process, fractional countercurrent extraction should be considered.

Major trade-offs and process limitations were examined quantitatively. Since the intent is to screen a number of possibilities for several hypothetical phase behaviors, simplifying assumptions were made to facilitate the calculations. Given a system, the operation of the crystallizer, extractor, and distillation column need to be rigorously optimized to obtain the best performance of the appropriate configurations. A sum-

Table 4. Summary of Configurations

Configuration	Phase Diagram	Comments
Class I with purge (Figure 2)	a, h	Values of B and D are relatively low.
Class I with 2 crystallizers (Figure 3)	h	A and B have high freezing temperatures.
Class I with column (Figure 4)	a	D makes B sparingly soluble
Class II with decanter and 2 crystallizers (Figure 7)	h	A and B have high freezing temperatures and A and D are partially miscible.
Class II with decanter (Figure 9)	b, c, d, f, g	Values of B and D are relatively low. Yield of B is sufficiently high
Class II with extractor (Figures 14, 15)	b, c, d, f	For most feed compositions, use crystallizer–extractor configuration.
Class II with fractional extractor (Figure 20)	b, c, d	Distribution coefficient is low.

mary of which configurations are appropriate for a specific phase behavior is given in Table 4.

Clearly, not all process alternatives are identified. Another possibility is to use supercritical extraction. Pressure or temperature swings can be used in these processes to control the extraction and regeneration steps. This alternative is most suitable to crystallizing compounds that must meet strict purity requirements. Additional process alternatives can also be generated when both the solvent A and the drowning-out agent are recycled as proposed by Weingaertner et al. (1991) to solution-mine salts.

The current design method can be improved in three areas. First, many industrial crystallization processes do not attain equilibrium; therefore, dynamic phase diagrams should be used in place of equilibrium diagrams (Hadzeriga, 1967). Second, the development of a method for higher dimensional systems should be investigated. Third, it is highly desirable to develop a companion experimental procedure for screening drowning-out crystallization designs. The process alternatives and the salient features of the corresponding phase diagrams identified in this study can help select a design with the minimum amount of experimental effort.

Acknowledgment

The support of the National Science Foundation (grant CTS-9220196) for this research is gratefully acknowledged. The graphic artwork of Ms. Pamela Stephan is greatly appreciated.

Notation

E = multistage extractor
α = relative volatility
ΔH_{cryst} = heat of crystallization, kJ/kg
ΔH_{vap} = heat of vaporization, kJ/kg
ΔT_{lm} = log mean temperature, °C

Subscripts

d = decanter
e = extractor

Literature Cited

Alfassi, Z. B., and S. Mosseri, "Solventing-Out of Electrolytes from Their Aqueous Solution," *AIChE J.*, **30**, 874 (1984).

Bemis, A. G., J. A. Dindorf, B. Horwood, and C. Samans, "Phthalic Acids," *Kirk Othmer Encyclopedia of Chemical Technology*, 3rd ed., Vol. 17, Wiley, New York, p. 732 (1982).

Berry, D. A., and K. M. Ng, "Separation of Quaternary Conjugate Salt Systems by Fractional Crystallization," *AIChE J.*, **42**, 2162 (1996).

de Bruyn, B. R., "Beitrag zur Kenntnis der Gleichgewichte mit zwei flüssigen Phasen in Systemen von einem Alkalisalz, Wasser und Alkohol," *Z. Phys. Chem.*, **32**, 63 (1900).

Douglas, J. M., *Conceptual Design of Chemical Processes*, McGraw-Hill, New York (1988).

Dorn, F., G. L. Smith, Jr., and J. C. McKenna, "The System $CuCl_2$-CH_3OH-$C_4H_8O_2$ at 30.0°C," *J. Chem. Eng. Data*, **10**, 195 (1965).

Dye, S. R., and K. M. Ng, "Bypassing Eutectics with Extractive Crystallization: Design Alternatives and Tradeoffs," *AIChE J.*, **41**, 1456 (1995a).

Dye, S. R., and K. M. Ng, "Fractional Crystallization: Design Alternatives and Tradeoffs," *AIChE J.*, **41**, 2427 (1995b).

Farrell, R. J., and Y. C. Tsai, "Nonlinear Controller for Batch Crystallization: Development and Experimental Demonstration," *AIChE J.*, **41**, 2318 (1995).

Fien, G. A. F., and Y. A. Liu, "Heuristic Synthesis and Shortcut Design of Separation Processes Using Residue Curve Maps: A Review," *Ind. Eng. Chem. Res.*, **33**, 2505 (1994).

Francis, A. W., "Ternary Systems of Liquid Carbon Dioxide," *J. Phys. Chem.*, **58**, 1099 (1954).

Francis, A. W., "Ternary Systems of Glycols," *J. Chem. Eng. Data*, **10**, 260 (1965a).

Francis, A. W., "Ternary Systems of Liquid Ammonia," *J. Chem. Eng. Data*, **10**, 329 (1965b).

Francis, A. W., "Ternary Systems of Liquid Sulfur Dioxide," *J. Chem. Eng. Data*, **10**, 45 (1965c).

Gomis, V., F. Ruiz, G. De Vera, E. Lopez, and M. Dolores Saquete, "Liquid-Liquid-Solid Equilibria for the Ternary Systems Water-Sodium Chloride or Potassium Chloride-1-Propanol or 2-Propanol," *Fluid Phase Equilib.*, **98**, 141 (1994).

Gomis, V., F. Ruiz, A. Marcilla, and M. del Carmen Pascual, "Equilibrium for the Ternary System Water + Sodium Chloride + Ethyl Acetate at 30°C," *J. Chem. Eng. Data*, **38**, 589 (1993).

Hadzeriga, P., "Dynamic Equilibria in the Solar Evaporation of the Great Salt Lake Brine," *SME Trans.*, **240**, 413 (1967).

Hanson, D. N., and S. Lynn, "Method of Crystallizing Salts from Aqueous Solutions," U.S. Patent 4,879,042 (1989).

Ho-Gutierrez, I. V., E. L. Cheluget, J. H. Vera, and M. E. Weber, "Liquid-Liquid Equilibrium of Aqueous Mixtures of Poly(Ethylene Glycol) with Na_2SO_4 or NaCl," *J. Chem. Eng. Data*, **39**, 245 (1994).

Jagadesh, D., M. R. Chivate, and N. S. Tavare, "Batch Crystallization of Potassium Chloride by an Ammoniation Process," *Ind. Eng. Chem. Res.*, **31**, 561 (1992).

Jones, A. G., and J. Mydlarz, "Continuous Crystallization of Potash Alumn: MSMPR Kinetics," *Can. J. Chem. Eng.*, **68**, 250 (1990).

Kolker, A. R., "Thermodynamic Modelling of Concentrated Aqueous Electrolyte and Non-Aqueous Systems," *Fluid Phase Equilib.*, **69**, 155 (1991).

Leonard, R. A., M. C. Regalbuto, D. B. Chamberlain, and G. F. Vandegrift, "A New Model for Solvent Extraction in Columns," *Sep. Sci. Tech.*, **25**, 1689 (1990).

Lo, T. C., M. H. I. Baird, and C. Hanson, *Handbook of Solvent Extraction*, Wiley, New York (1983).
Lozano, J. A. F., and A. Wint, "Double Decomposition of Gypsum and Potassium Chloride Catalyzed by Aqueous Ammonia," *Chem. Eng. J.*, **23**, 53 (1982).
Macchietto, S., O. Odele, and O. Omatsone, "Design of Optimal Solvents for Liquid-Liquid Extraction and Gas Absorption Processes," *Trans. Ind. Chem. Eng.*, **68**, 429 (1990).
Mersmann, A., and M. Kind, "Chemical Engineering Aspects of Precipitation from Solution," *Chem. Eng. Tech.*, **11**, 264 (1988).
McBride, T. K., and J. F. Brennecke, "Physicochemical Model of Solid-Liquid Solubilities Using NMR Measured Equilibrium Constants," *Fluid Phase Equilib.*, **85**, 191 (1993).
Minotti, M., M. F. Doherty, and M. F. Malone, "A Geometric Method for the Design of Liquid Extractors," *Ind. Eng. Chem. Res.*, **35**, 2672 (1996).
Mydlarz, J., and A. G. Jones, "Crystallization and Agglomeration Kinetics during the Batch Drowning-Out Precipitation of Potash Alum with Aqueous Acetone," *Powder Tech.*, **65**, 187 (1991).
Ng, K. M., "Systematic Separation of a Multicomponent Mixture of Solids Based on Selective Crystallization and Dissolution," *Sep. Tech.*, **1**, 108 (1991).
Pham, H. N., and M. F. Doherty, "Design and Synthesis of Heterogeneous Azeotropic Distillations—I. Heterogeneous Phase Diagrams," *Chem. Eng. Sci.*, **45**, 1823 (1990).
Pretel, E. J., P. A. López, S. B. Bottini, and E. A. Brignole, "Computer-Aided Molecular Design of Solvents for Separation Processes," *AIChE J.*, **40**, 1349 (1994).
Rajagopal, S., K. M. Ng, and J. M. Douglas, "Design of Solids Processes: Production of Potash," *Ind. Eng. Chem. Res.*, **27**, 2071 (1988).
Rajagopal, S., K. M. Ng, and J. M. Douglas, "Design and Economic Trade-Offs of Extractive Crystallization Processes," *AIChE J.*, **37**, 437 (1991).
Weingaertner, D. A., S. Lynn, and D. N. Hanson, "Extractive Crystallization of Salts from Concentrated Aqueous Solution," *Ind. Eng. Chem. Res.*, **30**, 490 (1991).
Zepeda, I. V., F. Lozano, and F. J. Garfias, "Liquid-Liquid Equilibrium for the Ternary System NaOH-H_2O-*t*-BuOH," *J. Chem. Eng. Data*, **24**, 287 (1979).
Zemaitis, J. F., Jr., D. M. Clark, M. Rafal, and N. C. Scrivner, *Handbook of Aqueous Electrolyte Thermodynamics*, Design Institute for Physical Property Data, AIChE (1986).
Zerres, H., and J. M. Prausnitz, "Thermodynamics of Phase Equilibria in Aqueous-Organic Systems with Salt," *AIChE J.*, **40**, 676 (1994).
Zhu, Y., L. B. Evans, and C. C. Chen, "Representation of Phase Equilibria Behavior of Antibiotics," *Biotechnol. Prog.*, **6**, 266 (1990).

Manuscript received July 5, 1996, and revision received Sept. 19, 1996.